

## Supplementary information:

### Ultrasound assisted one-step synthesis of Au@Pt dendritic nanoparticles with enhanced NIR absorption for cancer photothermal therapy

Yue Yang,<sup>a</sup> Mei Chen,<sup>a\*</sup> Yajiao Wu,<sup>a</sup> Peng Wang,<sup>a</sup> Yan Zhao,<sup>a</sup> Wenxiang Zhu,<sup>a</sup> Zhiling Song,<sup>b</sup> and Xiao-Bing Zhang<sup>a\*</sup>

<sup>a</sup> State Key Laboratory of Chemo/Biosensing and Chemometrics, College of Chemistry and Chemical Engineering, College of Materials Science and Engineering, Hunan University, Changsha 410082, PR China

<sup>b</sup> Key Laboratory of Optic-electric Sensing and Analytical Chemistry for Life Science, MOE, College of Chemistry and Molecular Engineering, Qingdao University of Science and Technology, Qingdao 266042, PR China

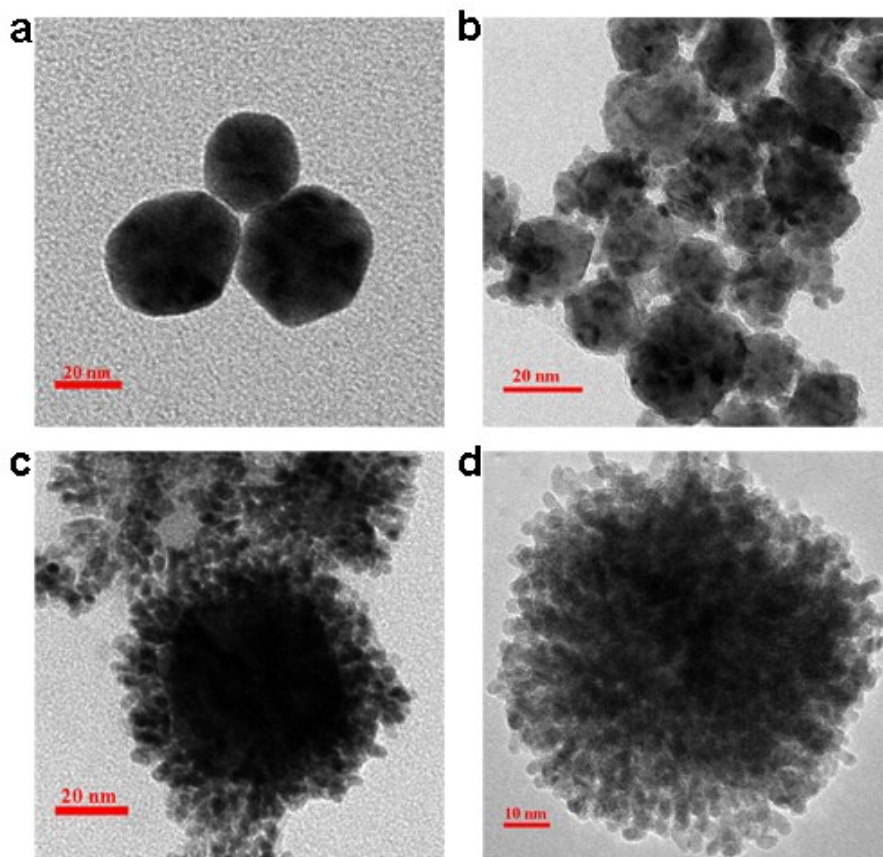


**Figure S1.** TEM images of (a) Au and (b-g) Au@Pt NPs with different Pt/Au molar ratios. The Pt/Au molar ratios are (a) 0.00, (b) 1.00, (c) 3.00, and (d) 4.00.

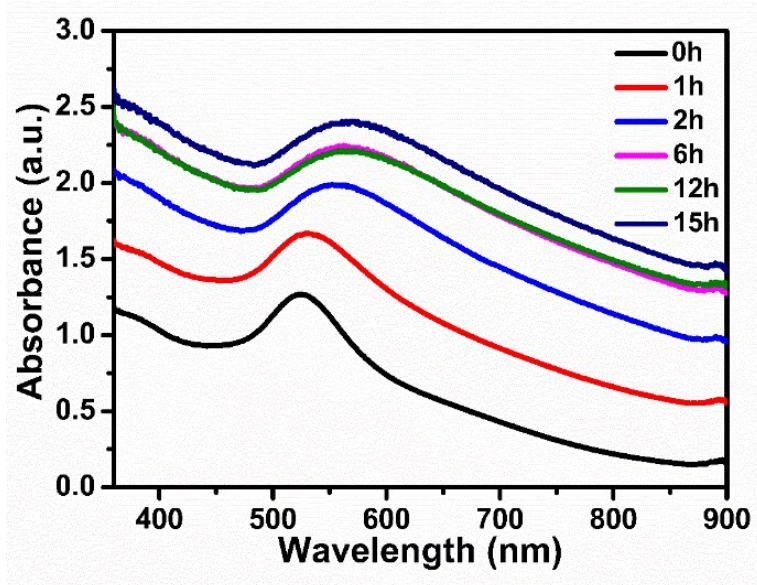


Figure S2. Time tracking of optical property of Au@Pt NPs.

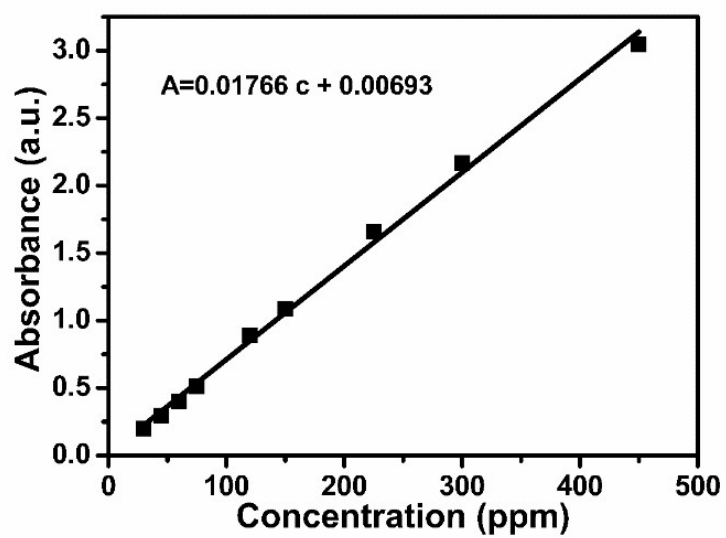


Figure S3. Optical absorption standard curve of Au@Pt NPs.

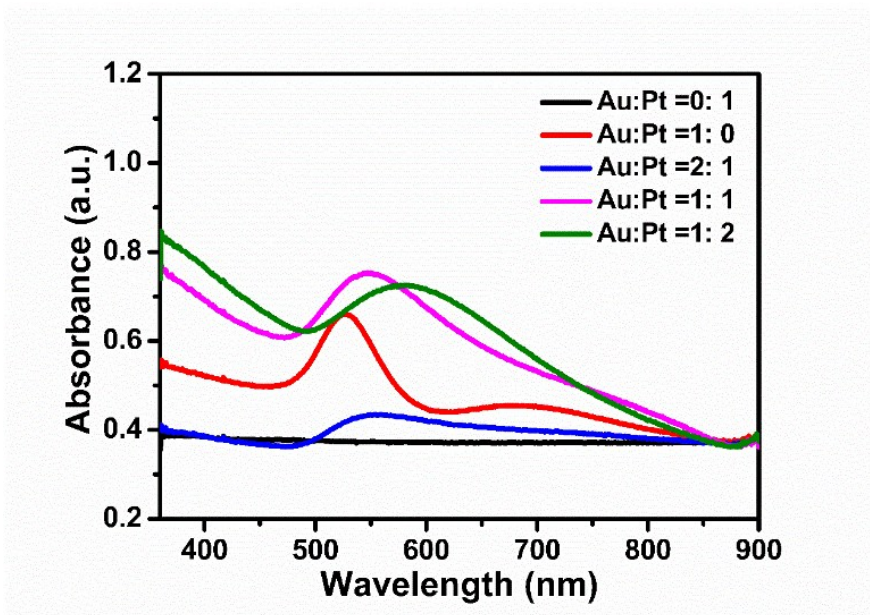


Figure S4. The optical property the Pt/Au ratio increased from 0 to 2.

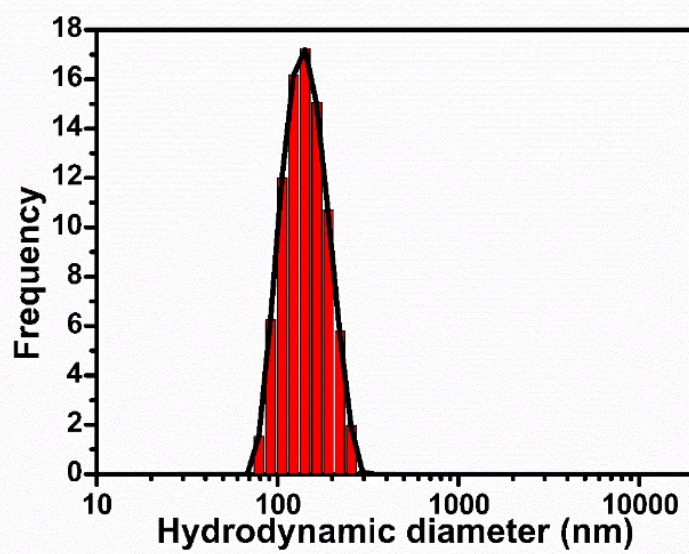
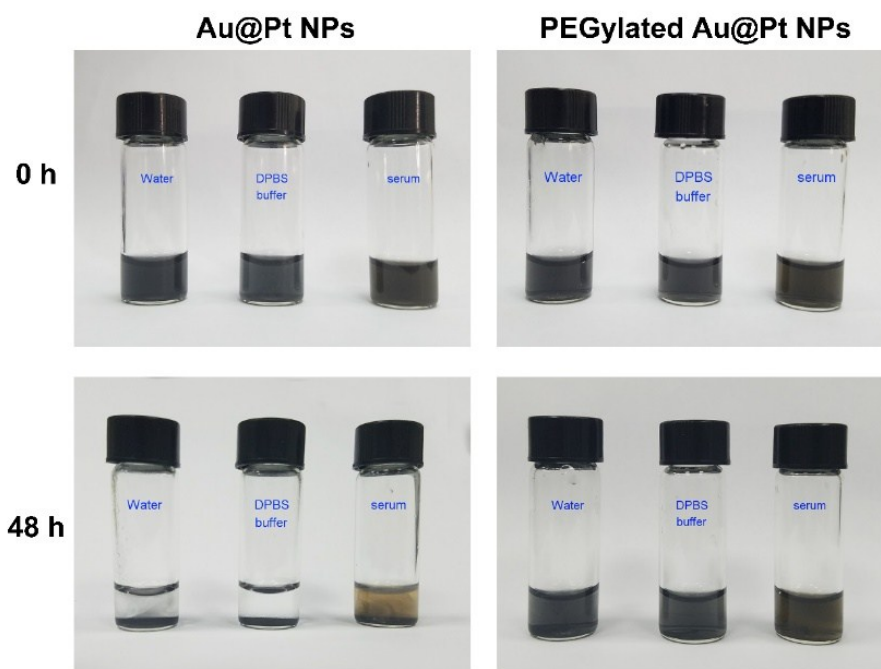
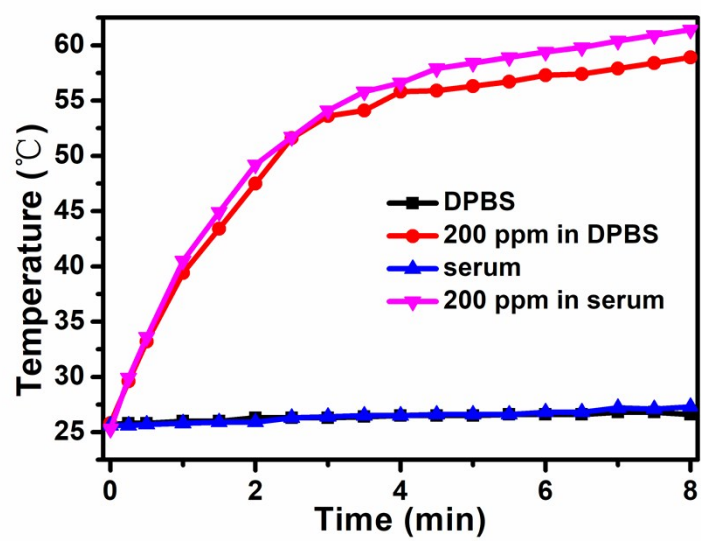


Figure S5. Hydrodynamic size distribution of Au@Pt NPs.



**Figure S6.** Digital photos of the Au@Pt NPs dispersion in different solutions before versus after PEG coating.



**Figure S7.** The temperature changes of Au@Pt NPs under an 808 nm laser irradiation in physiological conditions.



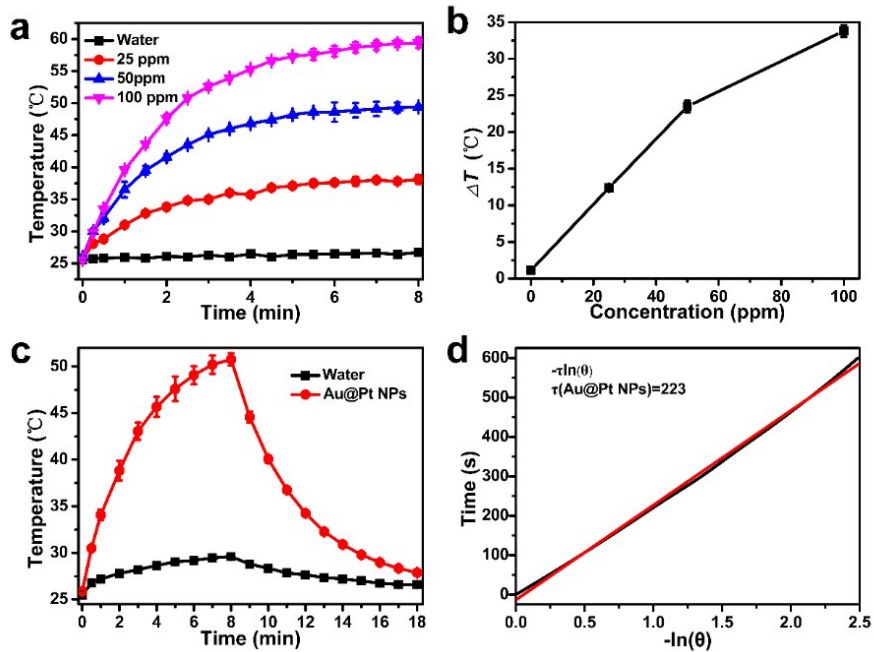


**Figure S8.** (a) The temperature changes of different concentration of PEGylated Au@Pt NPs under 808 nm laser irradiation at a power density of 0.8 W/cm<sup>2</sup>. (b) Relationship of the temperature change ( $\Delta T$ ) and concentrations of PEGylated Au@Pt NPs. (c) Temperature change curves of pure water and PEGylated Au@Pt NPs after being irradiated for 10 min in the beginning. (d) Time constant for heat transfer from the solution is obtained from the cooling stage.

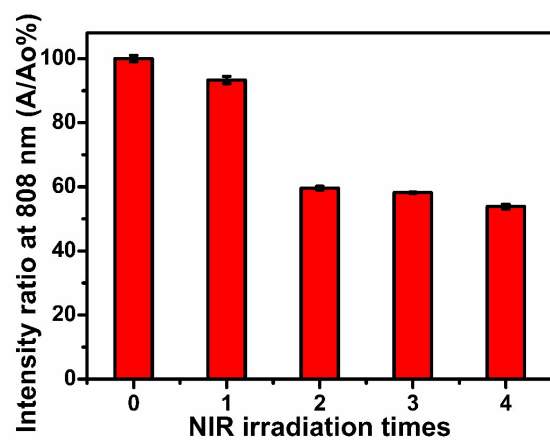


**Figure S9.** Variation of the absorption ratios at 808 nm ( $A/A_0\%$ ) of Au Nanorods after different irradiation cycles.

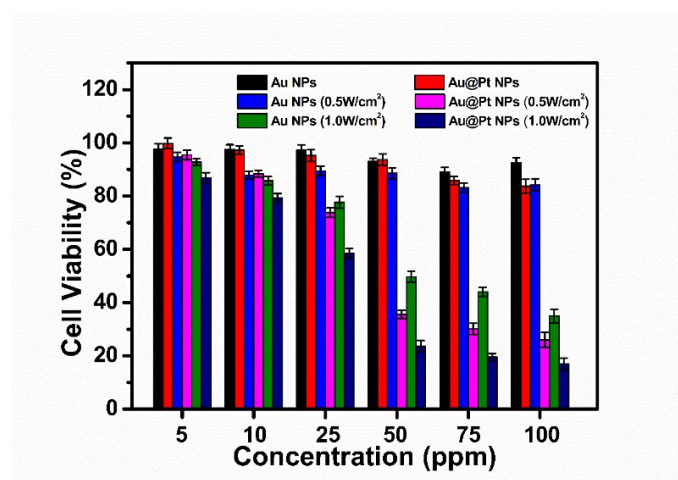


**Figure S10.** Cell viabilities of HeLa cells treated with PEGylated Au@Pt NPs without or with NIR laser.

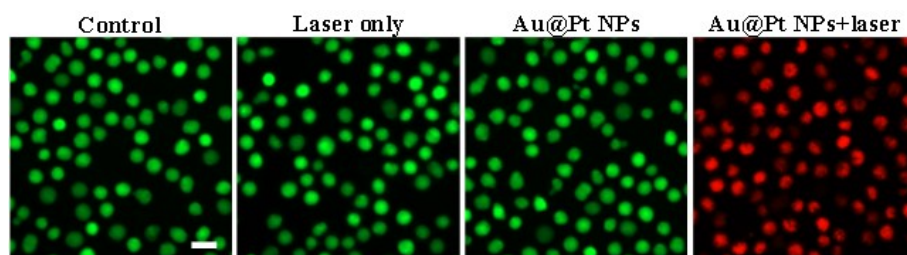


**Figure S11.** Fluorescent images of CCRF-CEM cells stained with Live/Dead Double Stain Kit, green fluorescence indicates live cells by calcein-AM, and red fluorescence indicates dead cells by PI. Scale bar, 50  $\mu\text{m}$ .

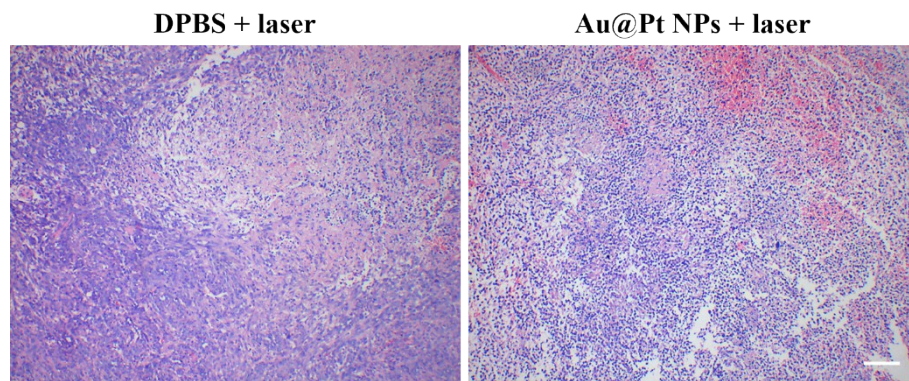


**Figure S12.** H&E-stained tissue sections of tumors harvested from mice with different treatments. Scale bar, 100  $\mu\text{m}$ .